Molecular Therapy
Oncology
Original Article

DARPin-fused T cell engager for adenovirus-mediated cancer therapy

Patrick C. Freitag,[1,8] Jonas Kolibius,[1,8] Ronja Wieboldt,[2] Remi Weber,[1,5] K. Patricia Hartmann,[1] Merel van Gogh,[3,6] Dominik Brücher,[1,7] Heinz Läubli,[2,4] and Andreas Plückthun[1]

[1]Department of Biochemistry, University of Zurich, Winterthurerstrasse 190, 8057 Zurich, Switzerland; [2]Laboratory for Cancer Immunotherapy, Department of Biomedicine, University Hospital and University of Basel, Hebelstrasse 20, 4031 Basel, Switzerland; [3]Department of Physiology, University of Zurich, Winterthurerstrasse 190, 8057 Zurich, Switzerland; [4]Division of Medical Oncology, University Hospital Basel, Petersgraben 4, 4031 Basel, Switzerland

Bispecific T cell engagers are a promising class of therapeutic proteins for cancer therapy. Their potency and small size often come with systemic toxicity and short half-life, making intravenous administration cumbersome. These limitations can be overcome by tumor-specific *in situ* expression, allowing high local accumulation while reducing systemic concentrations. However, encoding T cell engagers in viral or non-viral vectors and expressing them *in situ* ablates all forms of quality control performed during recombinant protein production. It is therefore vital to design constructs that feature minimal domain mispairing, and increased homogeneity of the therapeutic product. Here, we report a T cell engager architecture specifically designed for vector-mediated immunotherapy. It is based on a fusion of a designed ankyrin repeat protein (DARPin) to a CD3-targeting single-chain antibody fragment, termed DATE (*DA*RPin-fused *T* cell *E*ngager). The DATE induces potent T cell-mediated killing of HER2$^+$ cancer cells, both as recombinantly produced therapeutic protein and as *in situ* expressed payload from a HER2$^+$-retargeted high-capacity adenoviral vector (HC-AdV). We report remarkable tumor remission, DATE accumulation, and T cell infiltration through *in situ* expression mediated by a HER2$^+$-retargeted HC-AdV *in vivo*. Our results support further investigations and developments of DATEs as payloads for vector-mediated immunotherapy.

INTRODUCTION

Bispecific T cell engagers (BiTEs) have been extensively employed in cancer immunotherapy to physically link effector T cells to cancer cells.[1] This enforced interaction between the patient's immune system and the tumor cells ultimately results in T cell-mediated cell death of the tumor cells. The Food and Drug Administration (FDA) has approved this therapeutic approach for the treatment of hematological malignancies, while multiple approaches against solid tumors are currently at different stages of development.[2–4] Although various designs of BiTEs have been reported,[5,6] the most common format is based on a tandem arrangement of single-chain variable fragments (scFv) as described for Blincyto (blinatumomab), the first FDA-approved BiTE architecture targeting CD19 on B cells and CD3 on T cells.[5,7,8] However, conventional BiTE approaches face multiple difficulties: tandem scFv constructs are characterized by their small size of only 50–60 kDa, thus leading to rapid hepatic clearance from the blood circulation with a half-life of ~1.25 h in humans, as it is reported for blinatumomab.[9] The drug must therefore be continuously administered as an intravenous infusion, in contrast to most other antibody-based therapeutics carrying an Fc domain for half-life extension, which are administered only weekly or monthly.[10,11]

Administration of BiTEs via intravenous application results in a limited therapeutic window and reduced safety and clinical efficacy, especially when targeting solid tumors. Upon systemic application, the molecule encounters a multitude of T cells in the blood stream, while simultaneous interaction with cancer cells is limited. This represents a high risk for off-target activity as the BiTE may also interact with a plethora of different cell surface molecules other than the desired tumor antigen. Additionally, undesired on-target, off-tumor activity poses a serious risk for adverse effects during intravenous application.[12] For the majority of surface target proteins it has been shown that they are not solely expressed by the tumor cells, but to some extent also on healthy tissue,[13] making the expression level the key discriminator. In the case of HER2-targeting therapies, target expression in healthy heart and kidney tissue have raised serious concerns, as adverse effects like cardiotoxicity have been observed due to on-target activities in those tissues.[14] Additionally, the tumor core is hard to access for systemically administered protein therapeutics due to the high interstitial pressure and reduced blood flow in the tumor microenvironment.[15] Finally, it is likely that in many cases the immunosuppressive nature of the tumor microenvironment limits the

Received 13 November 2023; accepted 28 May 2024;
https://doi.org/10.1016/j.omton.2024.200821.

[5]Present address: Laboratory of Molecular Neuro-Oncology, Department of Neurology, Clinical Neuroscience Center, University Hospital and University of Zurich, 8091 Zurich, Switzerland

[6]Present address: Department of Medical Microbiology, University Medical Center Utrecht, 3584 CX Utrecht, Netherlands

[7]Present address: Vector BioPharma, 4051 Basel, Switzerland

[8]These authors contributed equally

Correspondence: Andreas Plückthun, Department of Biochemistry, University of Zurich, Winterthurerstrasse 190, 8057 Zurich, Switzerland.
E-mail: plueckthun@bioc.uzh.ch

efficacy of the BiTE.[16] For all these reasons, BiTEs have currently only been FDA-approved for hematological malignancies.

In situ production of T cell engagers at the tumor site offers an attractive opportunity to potentially overcome several of these difficulties and increase the therapeutic window by shifting the concentration from the systemic blood circulation toward the tumor site, thereby increasing the safety and efficacy of T cell engagers.

Retargeted or engineered adenoviral vectors have been used in various studies to establish potent *in situ* expression within the tumor microenvironment.[17–19] Particularly high-capacity adenoviral vectors of the serotype 5 (HC-AdV-C5) have proven to be capable of delivering multiple constructs with a payload capacity of up to 37 kb.[20–22] Our group has developed a trimeric adapter protein that binds quasi-covalently to the human AdV-C5 knob and effectively retargets the tropism toward tumor cells *in vivo*, leading to continuous expression of therapeutics from the tumor and subsequent secretion into the tumor microenvironment.[23–26]

Most recombinantly produced therapeutics are expressed and purified with rigorous analytic monitoring. This represents a strong contrast to *in situ* expression, which lacks the possibilities for quality control of the produced protein. The design and engineering of such biological therapeutics is therefore vital to reduce the risk of domain mispairing and/or aggregation caused by the architecture of multispecific antibody-derived proteins.[27,28] To the best of our knowledge, all current vector therapies have repurposed BiTEs that have been initially developed and optimized for recombinant production and systemic application, neglecting the risk of side product formation. Therefore, they usually require extensive purification and quality control protocols limiting their potential for *in situ* expression. Here, we present the development of a bispecific T cell engager that is optimized for the robustness required for *in situ* expression by tumor cells.

Designed ankyrin repeat proteins (DARPins) are a stable monomeric protein scaffold, used in a multimeric format, and currently under clinical investigation for intravenous injection targeting solid tumors.[29–33] Here, we report the combination of inherently stable DARPins with antibodies to engineer a DARPin-fused T cell engager (DATE, *DA*RPin-fused *T* cell *e*ngager), which is suitable for *in situ* expression by tumor cells. Replacing a single-chain variable fragment (scFv) of an antibody with a DARPin reduces the possible inter- and intra-molecular mispairing combinations that are known to afflict the variable domains of heavy (V_H) and light (V_L) chains in the context of tandem scFvs. This potentially improves the stability and solubility and ultimately reduces the possible inactive and/or nonspecifically interacting fraction of the T cell engager, which would otherwise need further downstream purification steps.[34]

We combined the HER2-binding DARPin G3[35] with an scFv that was generated from the antibody sequence of hXR32[36] connected by a flexible linker. Here, we report an HER2-CD3 targeting DATE that exhibits strong potency and selective cytotoxic T cell-mediated killing against different $HER2^+$ cancer cells. Targeted HC-AdV-mediated delivery of DNA encoding our DATE to $HER2^+$ cells yielded functional secretion and potent tumor cell killing *in vitro* and *in vivo* in tumor-bearing mice. We report compelling evidence suggesting that the DATE architecture could be explored further to improve T cell engager potency in vector cancer therapy for a more efficient and safe application.

RESULTS

DARPin-fused T cell engager DATE E08-G3 induces effector cell activity and dose-dependent tumor cytotoxicity

The DATE E08-G3 is a targeted immunotherapeutic agent designed for *in situ* expression and local accumulation. To ensure sufficient expression levels and to minimize potential misfolding, the DATE construct consists of a human serum albumin (HSA) signal peptide followed by the N-terminal anti-CD3 scFv connected with a short peptide linker to the C-terminal HER2-specific DARPin G3 (Figure 1A). Since functional expression by different mammalian cells is of importance for further applications in gene delivery vectors, we first assessed CHO-S cells as an expression host. Purity and integrity were verified by SDS-PAGE and SEC-HPLC analysis (Figure S1). Binding of DATE E08-G3 to both target molecules, CD3 and HER2, was examined via a sandwich enzyme-linked immunosorbent assay (ELISA) (Figure 1B). Simultaneous binding signals were solely detected in the presence of all three components, coated HER2, soluble DATE, and soluble CD3δε heterodimer. Furthermore, receptor-mediated cell surface binding was assessed via flow cytometry (Figure 1C). We used human lymphocyte Jurkat cells and the $HER2^+$ breast cancer cell line SKBR3 for our cell-binding assay and observed a distinct shift in fluorescence intensity compared with the cellular control without DATE (Figure 1C). To avoid any possible interference of an epitope tag, tag-less E08-G3 was detected via anti-DARPin rabbit serum and subsequently monitored with fluorescently labeled anti-rabbit antibodies.

Next, peripheral blood mononuclear cells (PBMCs) were used to assess effector cell-dependent, DATE-induced anti-tumor activity. After a 72-h incubation with 200 nM DATE, the majority of SKBR3 cells were killed in the presence of PBMCs, but not if effector cells were absent (Figure 1D). To examine DATE-induced T cell anti-tumor activity *in vitro*, we used a colorimetric XTT assay to determine metabolic activity as a surrogate for cell viability of the target cells in the presence of purified T cells from three different donors (Figure 1E). We monitored the DATE-induced, T cell-mediated cytolysis on the $HER2^-$ cancer cell line MDA-MB-468, on the $HER2^{low}$-expressing cell line MDA-MB-231, and on the three $HER2^{high}$-expressing cell lines MCF7, SKOV3, and SKBR3 (Figure 1E) with an effector-to-target cell ratio (E:T) of 2.5. While the $HER2^-$ cell line MDA-MB-468 was completely resistant to cell killing, $HER2^{low}$-expressing MDA-MB-231 cells displayed partial sensitivity. DATE E08-G3 engaged potent T cell-mediated killing of all three $HER2^+$ cancer cell lines in a dose-dependent manner even at picomolar concentrations. Importantly, even at high

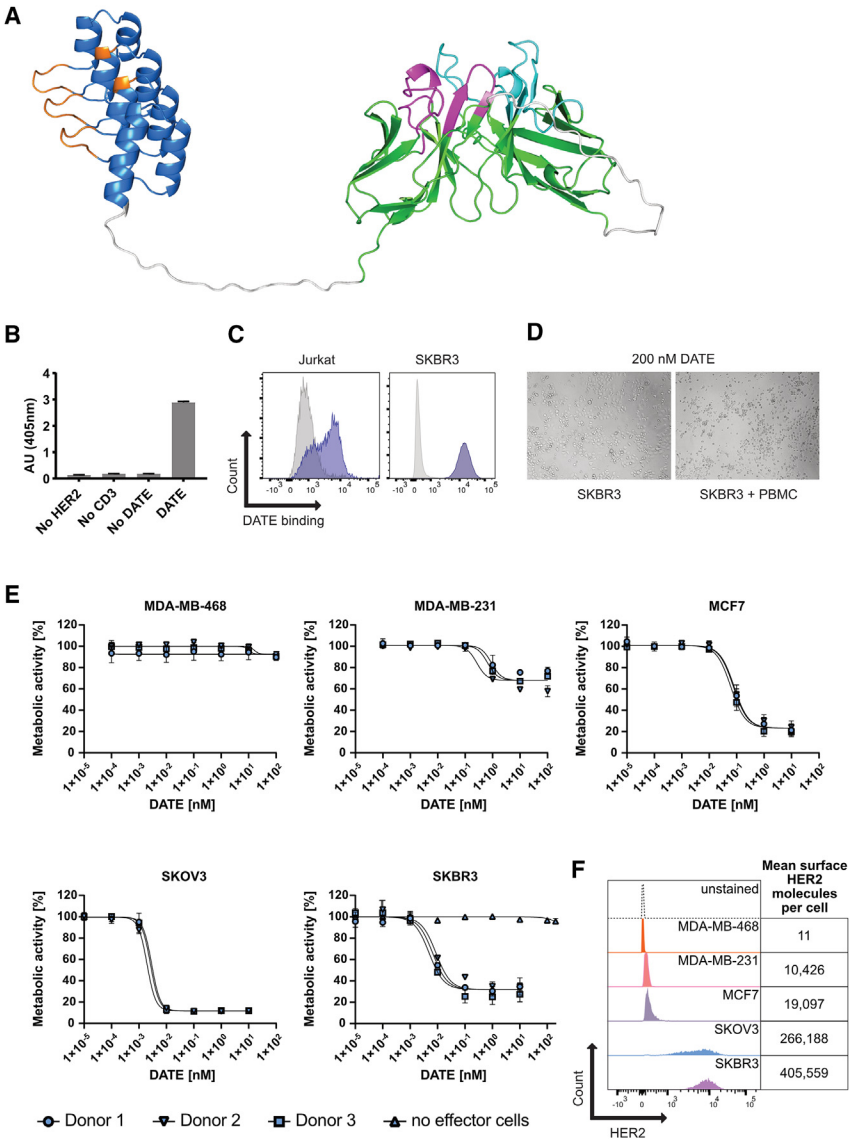

Figure 1. DATE targeting HER2 and CD3 induces HER2$^+$ cancer cell killing in the presence of human T cells

(A) Representative model of the three-dimensional structure of DATE E08-G3. The N-terminal, CD3-binding scFv (depicted in green, Complementary Determining Regions [CDRs] of V_H domain are shown in cyan and the CDRs of V_L are shown in magenta) linked to a C-terminal, HER2-binding DARPin (depicted in blue with the binding regions shown in orange). Linkers are depicted in gray. The structure was predicted using AlphaFold2. (B) Sandwich ELISA for simultaneous binding of CD3 and coated HER2 by DATE, including controls lacking indicated components. Bound CD3 in the sandwich was detected with FLAG-M2 antibody, followed by anti-rabbit IgG. (C) Cellular binding of DATE to Jurkat and SKBR3 cells measured by flow cytometry. DATE binding (purple histogram) was detected with anti-DARPin serum (produced in-house), and goat anti-rabbit IgG-AF555 (Thermo Fisher Scientific). Gray histograms represent cells without DATE binding. (D) Representative bright-field micrographs of HER2$^+$ SKBR3 cells after 3 days in the presence of 200 nM DATE with or without co-culture of PBMCs. (E) Effect of increasing concentrations of DATE on metabolic activity of different HER2$^-$ and HER2$^+$ cancer cell lines in co-culture with 2.5-fold excess of purified T cells (effector-to-target cell ratio [E:T] of 2.5:1) from three different donors, as measured by XTT assays. Dots represent mean of each donor ± SD (n = 3). Metabolic activity of SKBR3 cells was additionally assessed by XTT assays after treatment of cells with DATE for 3 days in the absence of purified T cells. (F) HER2 cell surface expression levels of different cancer cell lines analyzed via flow cytometry upon binding with a HER2-specific antibody. Cell surface levels of HER2 are shown relative to each other as histograms as well as the average of absolute receptor molecules per cell.

concentrations of 200 nM, the DATE did not exhibit any detectable cytotoxic properties in the absence of T cells as shown for SKBR3 cells (Figures 1D and 1E), pointing toward a T cell-dependent mode of action. To further investigate the HER2-specific activity of the DATE we quantified HER2 receptor cell surface levels for all tested cancer cell lines via flow cytometry (Figure 1F). Relative and absolute quantification using counting beads indicates that MDA-MB-468 cells do not display HER2 surface expression, while MDA-MB-231 and MCF7 cells show HER2^{low} and HER2^{medium} surface levels, respectively. SKOV3 and SKBR3 cells are characterized by high cell surface levels of HER2. The strong correlation between membrane-bound HER2 levels and DATE-sensitivity suggests that DATE E08-G3 indeed exerts an HER2-specific mode of action with high potency on HER2$^+$ cancer cells. Since intratumoral expression is expected to yield comparably low concentration levels, the high potency of DATE E08-G3 is a beneficial property for *in situ* expression.

DATE E08-G3 induces cytokine secretion in T cells

To confirm T cell activation and T cell-mediated cytolysis, we quantified the secretion of perforin, and the proinflammatory cytokines interferon γ (IFN-γ) and tumor necrosis factor α) (TNF-α. Healthy donor T cells were co-cultured with SKOV3, SKBR3, and MCF7 at an E:T of 2.5 for 72 h with increasing DATE concentrations (Figure 2). Secretion of all measured molecules correlated with the tumor cytotoxicity (Figure 1E) and DATE concentration. Furthermore, cytokine and perforin concentrations were at, or below the detection limit when tumor cell killing did not occur. Tumor cell killing, as well as

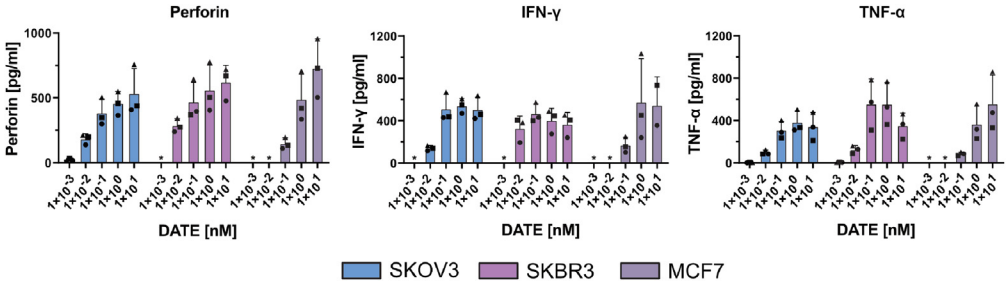

Figure 2. Secretion of effector proteins and cytokines upon T cell-mediated killing of cancer cells

ELISA quantification of secreted perforin, IFN-γ, and TNF-α after 72-h co-culture of a 2.5-fold excess of human T cells with different HER2^{+} cancer cell lines and increasing DATE concentrations. Individual symbols represent the average of technical replicates with the same donor. Bar graphs represent mean ± SD (* = below detection limit).

the secretion of perforin and cytokines were decreased in the HER2^{medium}-expressing cell line MCF7 and required higher DATE concentrations compared with the HER2^{high}-expressing cell lines SKOV3 and SKBR3.[37–39] This observation further highlights that the DATE-mediated anti-tumor activity shows HER2-specificity and is T cell-dependent.

Generation of retargeted high-capacity adenoviral vectors for targeted transduction

Adenoviral vectors belong to the most frequently applied viral vectors in clinical trials.[40] High-capacity human adenoviral vectors (HC-AdV) are the latest generation of adenoviral vectors, and they possess a large packaging capacity, allowing for multifactor approaches. HC-AdVs are devoid of all viral genes and can accommodate a transgene capacity of up to 37 kb,[41] opening the possibility to simultaneously encode a number of different payloads. We cloned the DATE E08-G3 gene into the HC-AdVs DNA and the vector was produced and purified via the iMATCH technology as previously described by our group.[20] Functionality and titers of the produced vectors were assessed by absorption (A_{260}), qPCR DNA quantification, and transduction assays on A549 cells.

Our group developed trimeric adapter molecules to redirect the tropism of HC-AdVs toward a new cell surface molecule. Briefly, a trimerized bispecific adapter blocks the natural tropism of HC-AdV-C5 by binding to the fiber-knob via a DARPin, while at the same time redirecting the specificity to a cell surface biomarker of choice by a retargeting moiety (Figure S2).[23,42–44] Blockage of the native interaction of the knob and tight binding to the knob is mediated by a C-terminally fused SHP trimerization domain (derived from lambdoid phage 21), which is extremely resistant to dissociation. This allows the DARPin to bind the trimeric fiber-knob as a clamp, which results in stable binding interaction without any detectable off-rate. At the same time, its binding eliminates the natural interaction between the fiber-knob and the AdV's primary attachment receptor coxsackievirus and adenovirus receptor (CAR).[23] Binding of the HC-AdV vectors to the retargeting adapter is achieved by incubating the trimer with the HC-AdVs for 1 h at 4°C and diluting the mixture for transduction. For proof-of-concept studies, we combined DATE-encoding HC-AdVs with an endotoxin-free HER2 retargeting adapter, which has been reported to successfully redirect adenoviral vectors toward HER2^{+}-tumor tissue in different *in vivo* experiments.[25,26,44]

Retargeted DATE-AdVs induce DATE expression and promote T cell-mediated tumor cell killing

As HC-AdVs are devoid of all adenoviral genes, no viral progeny is formed and instead, only the encoded payload is expressed. Thus, we wanted to test if functional DATE E08-G3 is expressed *in situ* from HC-AdV-transduced tumor cells and if T cell activation and T cell-mediated killing of HER2-expressing tumor cells occur, similarly to what was observed upon addition of recombinantly produced DATE to a co-culture of donor T cells and HER2^{+} tumor cells. Therefore, SKOV3 and SKBR3 were transduced with HER2-retargeted HC-AdVs encoding DATE (termed DATE-AdV) with a multiplicity of infection (MOI) of 1 and incubated for 16 h prior to co-culturing with PBMC-derived T cells for a further 72 h. In the absence of DATE-AdV, no reduction in metabolic activity was measured even after increasing E:T from 0 to 5 (Figure 3A). In line with our proposed mode of action, transduction of tumor cells with DATE-AdV results in a strong correlation between E:T cell ratio and reduced tumor cell viability and increased cytokine secretion, as indicated by XTT metabolic activity and cytokine ELISA (Figures 3A and 3B). Increased E:T ratios led to elevated levels of IFN-γ, TNF-α, and interleukin-2 (IL-2) secretion, correlating with the cytotoxic effect (Figure 3B). When tumor cells were transduced with a DATE-AdV MOI of 1, secretion of DATE was demonstrated by DATE ELISA (Figure 3C), with a slight increment upon increasing E:T ratio, presumably due to the increased cytolysis and release of cellular DATE. However, greater levels of DATE concentrations can be achieved if the cells are not killed by T cells, and the yield correlates with increasing MOI (Figure S3).

DATE-AdVs transduction of HER2 co-cultures only affects HER2-expressing cells

To confirm specific HER2-dependent effector cell-induced toxicity, we used mixed Flp-In-CHO cells expressing human HER2[23] and co-cultured them with their parental CHO cell line that does not express HER2 (Figure S4A). This co-culture was treated with DATE-AdV at an MOI of 10 and PBMC-derived T cells were added to a 10-fold excess compared with CHO cells. After 72 h, the HER2^{+} population decreased from 25.8% to 6%, while the HER2^{-} population

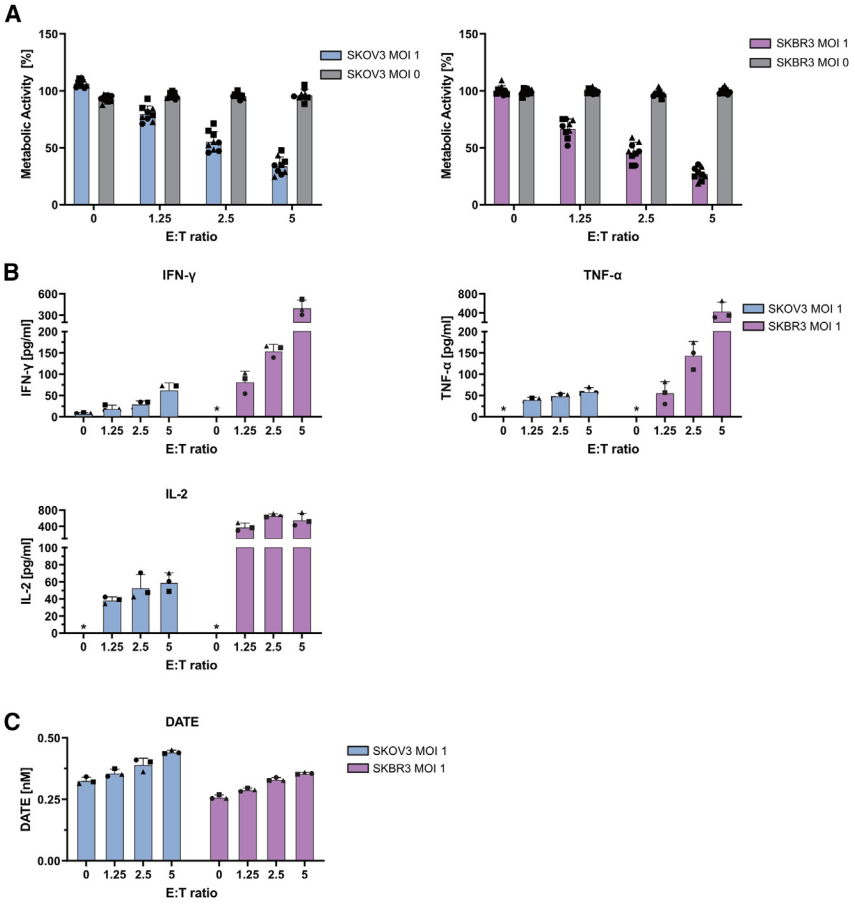

Figure 3. DATE-AdV transduction of tumor cells leads to expression of DATE and subsequent T cell-dependent tumor killing

(A) XTT measurements of cell viability determined as metabolic activity upon co-culturing SKOV3 or SKBR3 with increasing ratios of human T cells (E) to tumor cells (T) for 72 h. Tumor cells were transduced with retargeted HC-AdV encoding DATE E08-G3 (DATE-AdV) at an MOI of 1, 16 h prior to the addition of T cells. Individual symbols represent independent donors, replicates using the same donor are indicated by addition of the same symbol. (B) ELISA quantifications of secreted cytokines and (C) DATE concentration observed after transduction with DATE-AdV at an MOI of 1 and co-culturing tumor cells with increasing excess of T cells. Controls at an MOI of 0 and increasing effector to tumor cell ratio were below the detection limit of all quantified secreted cytokines. Individual symbols represent the average of technical replicates with the same donor. Bar graphs represent mean ± SD (* = below detection limit).

remained unaffected (Figure 4A, top graph). This reduction in the population size of $HER2^+$ cells was only observable upon addition of both DATE-AdV and effector cells to the co-culture (Figure 4A, bottom graph). Analysis of cell viability via XTT assay indicated a corresponding drop-in metabolic activity from 100% to 80% (Figure 4B). This suggests that the 20% reduction in overall cell viability results from a decrease in the number of HER2-expressing CHO cells (~26%–6%), highlighting the HER2-specific killing mechanism of the DATE. We can therefore attribute the cytotoxic effects to the HER2-expressing cells, excluding $HER2^-$ cells from cytolysis. Resistance toward DATE-induced T cell-mediated cell killing was also shown upon DATE-AdV transduction of $HER2^-$ cells in co-culture with PBMCs only, i.e., in the absence of $HER2^+$ CHO cells (Figure S4B). This corroborates our previously observed correlation between the potency of the DATE and the HER2 expression levels of different cancer cells (Figures 1E and 1F). Based on these results, we next wanted to evaluate the DATE technology *in vivo* and test for *in situ* payload expression.

DATE-AdV treatment results in relapse-free survival in 50% of tumor-bearing mice

To determine the *in vivo* efficacy of DATE secreted by tumor cells upon HC-AdV delivery, we administered three doses of 1.7×10^8 transducing units of HER2-retargeted HC-AdVs encoding either DATE E08-G3 (DATE-AdV) or GFP (GFP-AdV) intratumorally (i.t.) into NSG mice, which had previously been subcutaneously injected with $HER2^+$ SKOV3 cells for tumor establishment. Analogously, we administered three i.t. doses of 1 μg purified E08-G3 (DATE protein) into tumor-bearing NSG mice. A control cohort remained untreated (Figure 5A). According to prior work and our previously performed receptor quantification, each dosage of purified E08-G3 has a molar DATE to surface-bound HER2 excess of $5 \times 10^5 - 6 \times 10^7$ and should therefore be sufficient to cover all available HER2 molecules.[37,39]

All mice were reconstituted with 7×10^6 human T cells, isolated from two independent healthy donors, by intravenous injection (Figure 5A). Treatment groups were compared in terms of tumor growth, survival, T cell infiltration, DATE presence, and amount of delivered vector DNA for 91 days post tumor injection. No significant reduction in tumor growth was observed in GFP-AdV-treated mice compared to the untreated control group (Figure 5B). Injections of recombinant DATE protein resulted in delayed tumor growth, whereas DATE delivery by HC-AdVs and continuous *in situ* expression led to drastic reduction of tumor growth and tumor clearance (Figures 5B, 5C, and S5). Furthermore, 50% of DATE-AdVs-treated mice went into complete remission and remained tumor-free for over 90 days until the endpoint of the experiment (Figure 5D). This high rate of tumor-free mice was also confirmed in the pilot study with an independent third human T cell donor (Figures S6A and S6B). DATE-AdV treatment resulted in significantly prolonged survival, suggesting stable and lasting expression of DATEs and improved efficacy

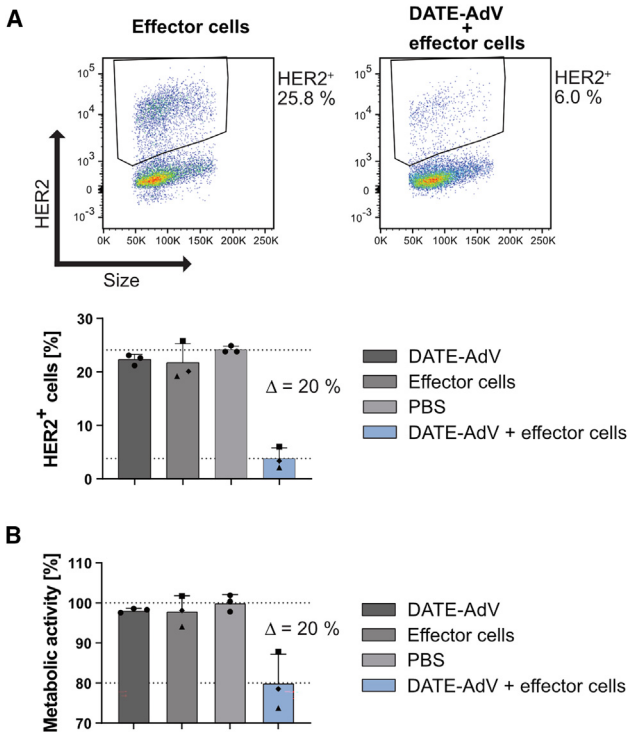

Figure 4. DATE-AdV induces specific killing of HER2⁺ cells

CHO-Flp-In cells with and without HER2 expression were mixed and transduced with DATE-AdV at an MOI of 10 and co-cultured with an E:T of 10:1 for 72 h. (A) Flow cytometry analysis of HER2 expression in the co-culture with (top, right graph) and without (top, left graph) transduction by DATE-AdV. Flow cytometric quantification of co-culture upon addition of DATE-AdV only, effector cells only, PBS control and DATE-AdV + effector cells (bottom graph) highlights that the decreased HER2⁺ population size correlates with the reduced metabolic activity depicted in (B). Bar graphs represent mean ± SD. (B) Determination of cell viability via XTT assay of HER2⁺ and HER2⁻ CHO-Flp-In co-cultures upon addition of DATE-AdV only, effector cells only, PBS control, and DATE-AdV + effector cells. Individual symbols represent single donors. Bar graphs represent mean ± SD.

by this continuous expression compared with injections of recombinant proteins (Figure 5D).

Both treatments, i.t. injection of DATE as recombinant protein as well as DATE-AdVs, resulted in detectable DATE accumulation in the tumor at the endpoint, as shown by immunohistochemical (IHC) analysis (Figure 6A). DATE-AdV treatment increased the presence of tumor-infiltrating T cells at the sampling time point, even though the tumor samples of DATE-AdV-treated mice were taken approximately 20 days after the tumor samples of the other groups. The infiltration and expansion of effector cells is suggested by co-localization of T cells and DATE, determined by immunohistochemistry. Furthermore, no T cell infiltration is visible in the untreated cohort and in mice after injection of GFP-AdVs, even though qPCR analysis confirmed successful GFP-AdV transduction of cells at the tumor site (Figure 6B). This confirms that T cell activation is indeed a direct result of the simultaneous binding of DATE to HER2⁺ tumor cells and T cells and not a consequence of vector-mediated immunogenicity. This conclusion is further corroborated by the observation that recombinantly produced and purified DATE results in a dose-dependent secretion of the cytokines IFN-γ and TNF-α and triggers the release of the cytolytic protein perforin from the purified T cells when they are co-cultured with HER2⁺ tumor cells (Figure 2), suggesting that potent T cell activation is also elicited in the absence of viral vectors.

A significant delay in tumor growth was also observed upon intravenous injection of DATE-AdV (Figures S7A and S7B). Furthermore, increased concentrations of the proinflammatory cytokine TNF-α, secretion and localization of DATE, and infiltration by T cells were confirmed by tumor tissue analysis via ELISA and immunohistochemistry (Figures S7C and S7D). Quantification of normalized immunofluorescent signals obtained from IHC analysis confirms that i.t. injection of DATE-AdV indeed induces sustained DATE expression and secretion into the tumor microenvironment resulting in a large number of T cells localized to the tumor (Figure S8). In comparison, administration of recombinant DATE or intravenous injection of DATE-AdV result in reduced levels of DATE within the tumor and consequently in a decreased T cell count, whereas untreated and GFP-AdV-treated animals do not display DATE expression or T cell infiltration. Neither application of HC-AdVs nor of purified protein led to significantly elevated alanine aminotransferase (ALT) levels in the serum compared with the control group, suggesting no liver toxicity in this mouse model (Figure S9).

Altogether, these data show that DARPin-fused T cell engagers (DATEs) are a suitable protein architecture for targeted adenoviral vector therapy, local secretion, and T cell engagement, with a potent and sustained therapeutic effect in solid tumors *in vivo*. Most importantly, this protein format shows improved efficacy over direct injection of the same agent when delivered by HC-AdV, as it is produced locally over a long period of time.

DISCUSSION

This study reports the development of DARPin-fused T cell engagers (DATE) as a new bispecific protein architecture for functional and potent *in situ* expression by vector therapy. We showed that a HER2-CD3 targeted DATE mediates T cell-dependent killing of HER2⁺ cells as recombinantly produced protein. Furthermore, we demonstrated targeted delivery of a DATE-encoding payload via HC-AdV and successful expression and secretion from different tumor cells. This subsequently promoted T cell-mediated killing of HER2⁺ tumor cells in a dose-dependent fashion of DATE and T cells. In combination with our previously developed retargeting strategy,[23] the HC-AdV successfully transduced the ovarian cancer cells SKOV3 in an NOD/SCID xenograft mouse model. Continuous *in situ* expression resulted in local accumulation of the DATE within the tumor for up to 45 days after the last vector injection, followed by T cell infiltration leading to tumor mass reduction and significant survival benefit.

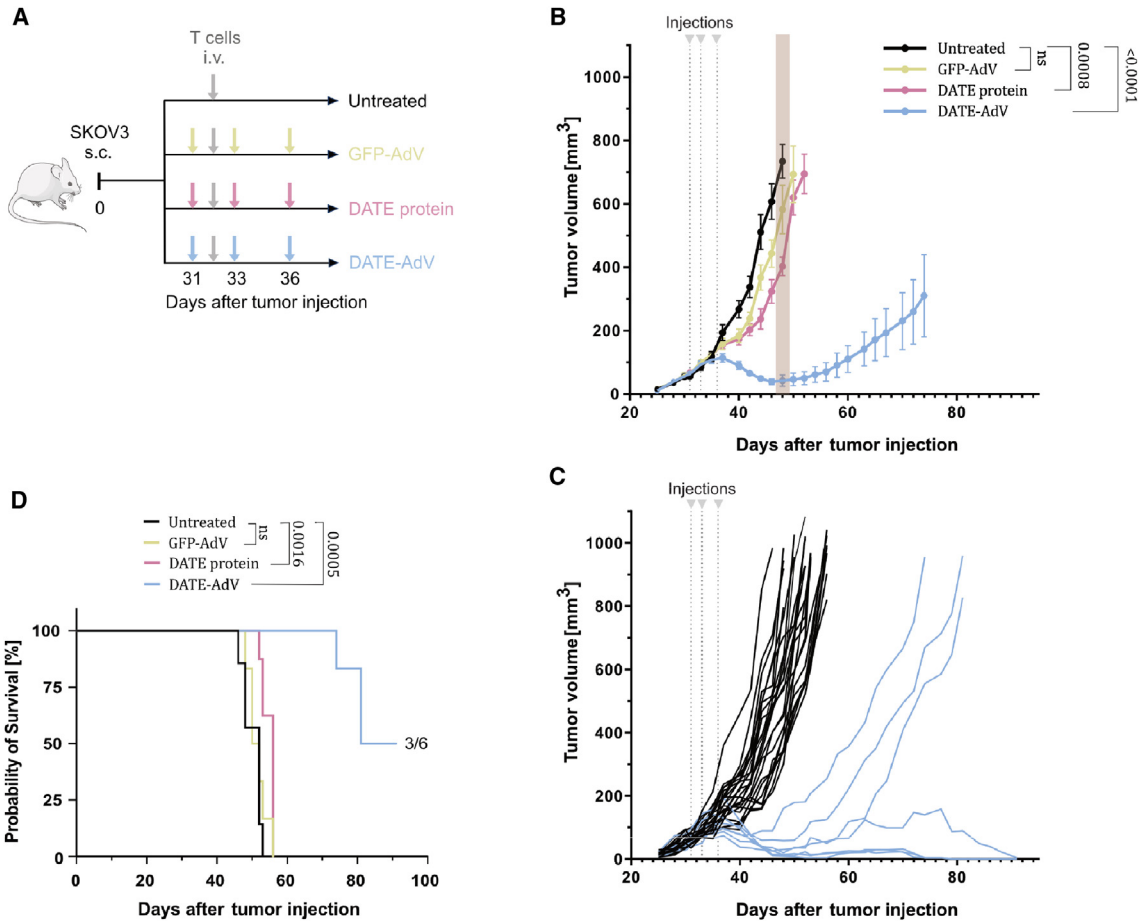

Figure 5. *In vivo* efficacy of DATE-AdVs in tumor-bearing NSG mice reconstituted with human T cells

Subcutaneous SKOV3 tumor-bearing mice were treated with three intratumoral injections of the indicated constructs and a single, intravenous injection of 7 × 10^6 human T cells. T cells were derived from two different healthy donors. (A) Depiction of treatment scheme. NSG mice were subcutaneously injected with human ovarian HER2-expressing SKOV3 cancer cells and treated intratumorally with therapeutics or were left untreated once the tumors reached a tumor volume of 30–100 mm^3. Mice received three consecutive injections (indicated by arrows) of DATE-AdV, GFP-AdV (each 1.7 × 10^8 transducing units), or 1 μg of recombinantly produced DATE and were reconstituted with human T cells 1 day after the first injection of therapeutics. (B) Injections of recombinantly produced DATE or of DATE-AdV resulted in significantly reduced average tumor size. DATE-AdV showed strongest anti-tumoral effect. Statistical comparison between groups was performed on day 48 after tumor injection (indicated by brown bar). (Mixed effect analysis with Tukey's multiple comparison test, n = 6–8 animals per group, dots represent mean ± SD). (C) Tumor growth of individual mice was substantially inhibited upon DATE-AdV treatment (light blue) compared with the all-other treatment groups (black), resulting in complete remission after 91 days in 50% of the DATE-AdV-treated animals. (D) 50% of DATE-AdV-treated mice show complete tumor-regression and greatly improved overall survival. (Log rank [Mantel-Cox] test, ns = $p > 0.05$).

Previous preclinical and clinical studies have extensively demonstrated the safety concerns of HER2-targeting therapies.[14] Many tumor-associated antigens, including the HER2 antigen, are not solely a tumor antigen but are also expressed in healthy tissues. On-target, off-tumor cytotoxicity and T cell activation can therefore result in potent elimination of healthy tissue and severe side effects.[14,45] Thus, establishing target- or organ-specific accumulation within the tumor microenvironment and reducing systemic concentration is essential for limiting undesirable side effects from T cell engager and vector therapy in cancer patients.[19,46,47] To maximize the therapeutic window and circumvent these risks we have employed a double lock system comprising (1) target cell-specific transduction resulting in continuous local secretion and (2) accumulation of the target-specific and small DATE resulting in highly specific tumor cell lysis. The low hydrodynamic radius compared with IgG formats is presumably the reason for low systemic concentrations and thus reduced off-site effects due to the rapid clearance of BiTE constructs from the bloodstream.

The $HER2^+$-specific killing, shown by $HER2^+$ and $HER2^-$ co-cultures transduced with DATE-AdVs and the correlation of HER2 expression levels and sensitivity toward DATE E08-G3 treatment, supports the specificity of *in situ* produced E08-G3 by DATE-AdV virotherapy. Maximal DATE anti-tumor activity was already observed at

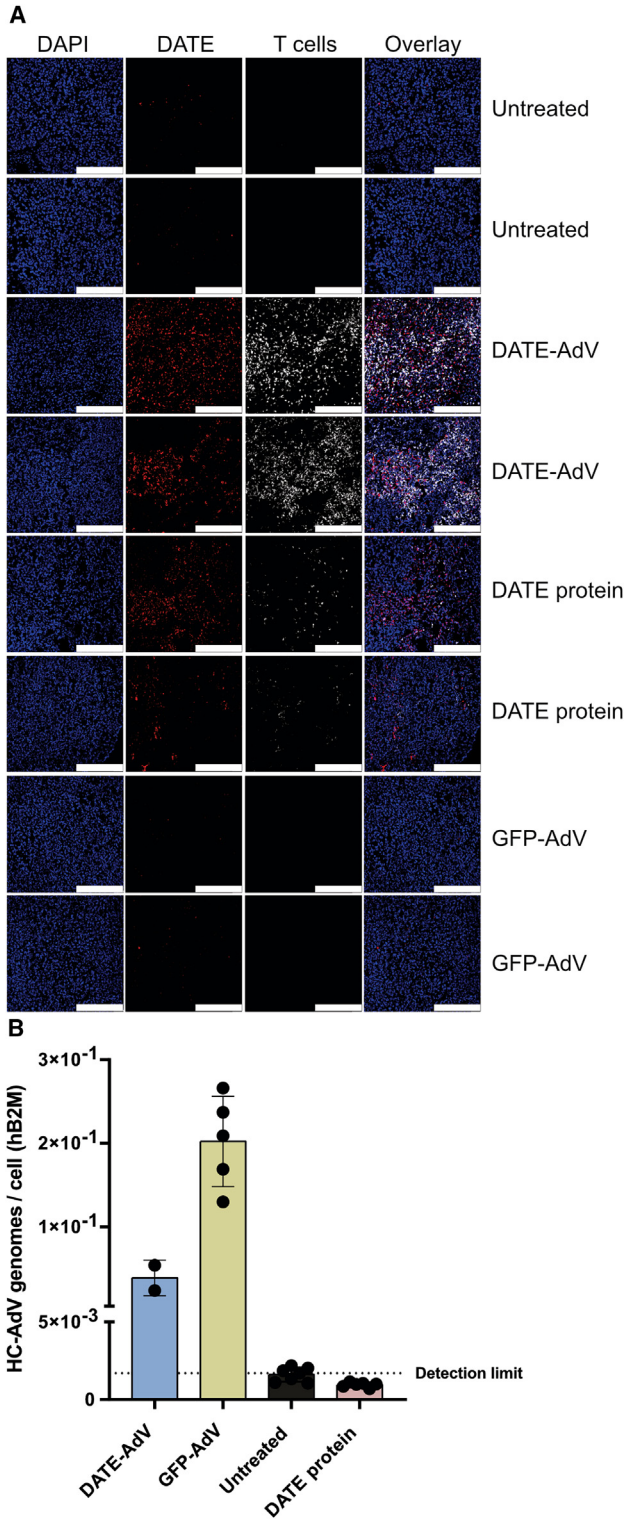

Figure 6. Tumor tissue analysis of treated mice indicates potent DATE *in situ* expression mediated by DATE-AdV transduction and T cell accumulation in the tumor

(A) Representative immunofluorescence images of tumor tissue slices (harvested at endpoint and embedded in optimal cutting temperature compound [OCT]) stained for DATE (red) or T cells (light gray) and counterstained with DAPI (blue) for nuclei staining. Scale bar, 250 μm. Two representative images are shown of each treatment group. (B) qPCR analysis of vector DNA in tumor tissue at endpoint. Bar graphs represent mean ± SD.

picomolar concentrations, highlighting the low amounts required for efficient anti-tumoral effects. The high potency of the described T cell engager therefore only requires low transduction rates and hence potentially allows a reduced dosage of administered viral particles. We thus want to emphasize the importance of taking these molecular properties into consideration during future designs of DATEs for *in situ* expression.

Here, we show that rational design of new T cell-engaging molecules can be useful to generate highly efficacious proteins for anti-cancer therapy. Similar to trastuzumab, the DARPin G3 as part of the DATE, binds to the HER2 subdomain IV, which is in close proximity to the cell membrane.[48] In the context of bispecific IgGs this has been shown to be beneficial to increase the efficacy of T cell engagers.[49] Furthermore, retargeted HC-AdVs have been used for immunotherapeutic combination therapies encoding several cytokines to modulate the immune status of the tumor microenvironment.[20,22] These combinations could potentially increase efficacy and can also be linked to DARPin-targeting moieties, as DARPins have here been shown to be suitable targeting molecules for *in situ* expression.

Although multiple engineering approaches aim to improve stability and aggregation behavior of scFvs,[34,50–52] scFv-scFv fusions exhibit the additional disadvantage of domain reassociations, mispairing, and thus interference with binding and activity. DARPins are a class of synthetic and stable binding proteins that are usually expressed in *E. coli*.[32] By designing a fusion protein of an N-terminal, mammalian scFv protein linked to a highly stable DARPin, intra-molecular dissociation and reassociation have been made inherently impossible and inter-molecular interferences less likely. Thus, we hypothesize that the functional fraction of the effector molecule is increased, potentially allowing reduction of the required dosage of the delivery vector for efficacious *in situ* expression.

Different oncolytic viruses have been combined with immunotherapeutic agents[53,54]; however, as oncolytic viruses are designed to target cancer tissue and to selectively produce viral progeny in the tumor cells, retargeting strategies with this vector class are limited and mostly restricted to tumor cells. Using non-replicative vectors such as HC-AdVs instead offers more general retargeting strategies. These could include targeted transduction of the tumor microenvironment such as tumor-associated fibroblasts[44] or tumor adjacent healthy tissue without destroying it. Since increased DATE concentrations have been measured to be secreted by transduced cells without killing the producer cells, transduction of local non-cancerous cells could potentially further prolong the secretion of the DATE, resulting in increased therapeutic effects.[44] Continuous

production via viral therapy circumvents the need of continuous administration by recombinant protein therapy while also inverting the concentration gradient from high systemic to high tumor concentrations.[26]

It is relevant to consider shortcomings associated with animal models that lack a fully functional immune system and cross-reactive binding targets. These models have therefore an inherent deficiency in recapitulating the tumor and immunological microenvironment. Future studies deploying immunocompetent hosts that feature mouse cross-reactive targets will be necessary for each specific DATE to be deployed for therapeutic applications.[55] Furthermore, efficacy has been shown upon intravenous injection, although inferior to the intratumoral injection. For future developments, we suggest improving the efficacy of HC-AdV-mediated immunotherapy by taking advantage of the large (37 kb) transgene capacity of these vectors. The potency could be increased by combining DATEs with additional targeted immunotherapeutics, and potential off-target expression could be managed by introducing specific promoters and/or transcription factors combined with microRNA, allowing improved efficacy upon systemic application.

Taken together, the current work represents a proof-of-principle study for DATEs as a suitable protein architecture for *in situ* expression and anti-tumor vector therapy. The presented results are encouraging and demonstrate the potential of DATEs as a tool for potent vector-based immunotherapy.

MATERIAL AND METHODS

Expression and purification of DATE E08-G3

CHO-S cells were diluted in fresh CHOgro medium (Mirus Bio, Madison, WI) (containing 4 mM L-glutamine, 0.3% poloxamer 188) at a density of 2×10^6 cells/mL. Sixteen hours later the cells were resuspended in fresh CHOgro medium (4×10^6 cells/mL, 250 mL, TubeSpin Bioreactor 600) and 1.25 μg/mL of DNA, 3 μg/mL of PEI and 72 μg/mL valproic acid were added sequentially under continuous swirling. Cells were incubated for 7 days at 120 rpm, 5% CO_2, 31°C. Next, the cells were separated from the supernatant by a centrifugation step (3,000 × *g*, 20 min, 4°C) followed by a filtration step (0.22 μm, Stericup Quick ReleaseGP) and the supernatant was dialyzed against PBS, pH 7.4 (4°C). Expressed protein was purified by NiNTA beads, washed with five column volumes of PBS, pH 8.0, supplemented with 20 mM imidazole and 10% glycerol, followed by five column volumes of TBS, pH 8.0, containing 50 mM Tris-HCl and 500 mM NaCl. Washed protein was eluted using TBS, pH 8.0, supplemented with 500 mM imidazole. Eluted protein samples were incubated together with 3C protease (8 μg/mL) and dialyzed in 20 mM HEPES 20 mM NaCl, pH 8.0 ($1{:}8 \times 10^9$ dialysis, 4°C). The dialyzed protein was then applied to a Mono Q 5/50 GL anion exchange column (Cytiva, Marlborough, MA). Concentration of purified protein samples was determined by measuring the absorbance at 280 nm (NanoDrop One Microvolume UV/Vis Spectrophotometer, Thermo Fisher Scientific, Waltham, MA).

Analytical HPLC SEC

Analytical size exclusion chromatography was performed by running an AdvanceBio SEC 300 Å column on a 1260 Infinity HPLC system (Agilent Technologies, Santa Clara, CA). The column was calibrated with an AdvanceBio SEC 300 Å Protein Standard (Agilent Technologies). Protein samples were injected at a flow rate of 0.15 mL/min. UV absorbance was monitored at 280 nm.

Cell culture

All human cell lines were cultured in Tissue Culture Flasks 75 cm^2 with RPMI 1640 (Gibco, Waltham, MA) supplemented with 10% (v/v) heat-inactivated fetal calf serum (FCS), and 1% (v/v) penicillin/streptomycin (Sigma-Aldrich, St. Louis, MO) at 37°C and 5% CO_2 and all cell counts were determined using a CASY TT cell counter. MDA-MB-468, MDA-MB-231, MCF7, SKOV3, and SKBR3 cells were cultured in Dulbecco's Modified Eagle Medium (Sigma-Aldrich), supplemented with 10% (v/v) FCS, 1% (v/v) penicillin/streptomycin (Sigma-Aldrich). Parental CHO cells and Flp-In-CHO cells expressing human HER2 were cultured in Ham's F-12 medium (Thermo Fisher Scientific), supplemented with 10% (v/v) FCS, 1% (v/v) penicillin/streptomycin (Sigma-Aldrich), and were already described elsewhere.[23] Fifty milliliters of buffy coat samples from multiple donors were used for PBMC isolation. Each donor was purified separately by Ficoll gradient centrifugation and subsequently frozen at −80°C. For effector-mediated killing assays, PBMCs were prepared one day in advance by resuspension in IL-2-lacking complete RPMI at a cell density of 5×10^5 cells/mL.

Sandwich ELISA assay

A 384-well flat bottom polystyrene microplate was coated with 25 μL/well 100 nM HER2 (Abcam, Cambridge, UK) in PBS for 2 h at 4°C. The coating solution was removed by inversion of the plate, and the plate was blocked with 120 μL/well of PBS supplemented with 1% Tween 20 (v/v) and 0.2% (w/v) bovine serum albumin (BSA). The plate was washed three times with 120 μL/well PBS containing 1% Tween 20. Twenty-five microliters per well of 100 nM DATE in PBS was applied and incubated for 1 h at 4°C. After three more washing steps, 100 nM CD3δ, CD3ε heterodimer (Sino Biological, Beijing, China) was added in PBS for 1 h at 4°C. The bound CD3 was then detected using its FLAG tag by an FLAG-M2 antibody (Cell Signaling Technology, Danvers, MA) followed by anti-rabbit IgG (Thermo Fisher Scientific) coupled to alkaline phosphatase. After 1 h incubation at 4°C, the plate was washed again three times and pNPP substrate solution was added. After a 30-min incubation at 4°C, the absorbance measurement was performed using an Infinite M1000 microplate reader (Tecan Group, Männedorf, Switzerland) at an absorbance wavelength of 405 nm with a reference measurement at 540 nm.

Effector cell-mediated killing assays

A total of 4,000 target cells were seeded in a 96-well microplate with culture medium 24 h prior to addition of effector cells. If viral vectors were used, target cells were transduced 6 h after seeding. If purified protein was analyzed, fresh culturing medium with the respective

sample and T cells or PBMCs were added and incubated for 72 h. In case of virally delivered DATE E08-G3, T cells or PBMCs were added without exchange of media. After 3 days, the supernatant was separated from the adherent cells. The adherent cells were used for the cell viability assay and the supernatant was centrifuged to separate the T cells or PBMCs from medium, which in turn was used for the cytokine assay.

Cell viability assay

Cell viability was assessed using XTT (Roche, Basel, Switzerland) following the manufacturer's protocol. The XTT reagent was incubated with the cells for 5 h before measuring absorbance at (473 nm, ref. 670 nm) using an Infinite M1000 instrument (Tecan Group). Dose-response curves were fitted to the XTT data by a least-squares fit.

Analysis of HER2 cell surface expression

HER2 cell surface expression was analyzed via flow cytometry by antibody staining as follows. Cells were harvested by trypsinization, washed with ice-cold FACS buffer (PBS containing 1% [w/v] BSA and 0.1% [w/v] NaN_3), and resuspended in ice-cold FACS buffer to proceed with the antibody staining. A total of 1×10^6 cells were incubated with mouse anti-HER2-AF647 antibody (BioLegend, San Diego, CA, 324412, 1:200 dilution) for 20 min on ice. Cells were then washed with ice-cold FACS buffer and fixed with fixation buffer (PBS containing 4% [w/v] paraformaldehyde [PFA]) for 15 min at room temperature (RT). After a final wash step, cells were resuspended in FACS buffer and stored at 4°C until analysis at a BD FACSymphony 5L flow cytometer (BD Biosciences, Franklin Lakes, NJ). Flow cytometry analysis was performed using FlowJo software (BD Biosciences).

Quantitative HER2 cell surface determination was performed using the Quantitative Analysis Kit QIFIKIT (Agilent Dako, Santa Clara, CA). HER2 receptor quantification was performed following the manufacturer's instructions using mouse anti-HER2 antibody (BioLegend, 324401) and mouse anti-IgG1 kappa antibody (BioLegend, 400101).

Cytokine assay

The cytokine assays were performed using human ELISA Kits (Thermo Fisher Scientific) as described by the manufacturer's instructions. However, all measurements were performed using 384-well plates and volumes were reduced accordingly. Absorbance measurements were performed using an Infinite M1000 instrument (Tecan Group).

Viral vector production and quantification

First, DATE cDNA was cloned into the pUni plasmid and then the DATE expression cassette was further subcloned into the pC4HSU[56] plasmid using the iMATCH technology.[20] DATE expression was driven via the constitutive CMV promoter. In short, the cell line 116 was transfected with the linearized pC4HSU genome containing the HAdV-C5 packaging signal and co-infected with HAdV-C5 helper virus (HV) (encoding four mutations in the HVR7 region [I421G, T423N, E424S, and L426Y][25]) for production of capsid-modified HC-AdV particles. Seventy-two hours post-transfection, the initial passage was harvested and the HC-AdV titer was sequentially increased over several passages by harvest of the producer cells, release of produced HC-AdV via three consecutive cycles of freeze-thawing and re-transduction of new producer cells together with new HVs. Thereby, the titer was increased over multiple passages, as described elsewhere in detail.[20,57] HC-AdV particles were then purified and empty particles and remaining HVs were removed via two CsCl gradients and ultracentrifugation at 250,000 × *g*, followed by dialysis of recovered vector against 150 mM NaCl, 20 mM HEPES, 1 mM $MgCl_2$, pH 8.1.[20,57] Functionality and concentrations of the produced vectors were determined by absorption (A_{260}) and transduction assays on A549 cells. To determine the transducing titer, 50,000 A549 cells were seeded in a 24-well microplate 24 h prior to transduction of cells with 3 μL of purified vector. Two hours later, A549 cells were harvested by trypsinization and the cell pellet (800 × *g*, 5 min, 4°C) was washed once with PBS. Total DNA of transduced cells was extracted using a Genekam DNA isolation kit (Genekam, Germany). The transducing titer of the tested vector was quantified via multiplex-qPCR with specific primers and double-quenched probes for HC-AdV (5′-TCTGC TGGTTCACAAACTGG-3′, 5′-TCCTCCCTTCTGTCCAAATG-3′, 5′-FAM-CGCCTTCTCCTGCATCCCGA-3′) and HV (5′-GTGA TAACCGTGTGCTGGAC-3′, 5′-CAGCTTCATCCCATTCGCAA-3′, 5′-HEX-TCCGCGGCGTGCTGGACAGG-3′) (IDT, Coralville, IA) using the total DNA isolate as a template. Genomic HC-AdV titer and HV contamination was directly quantified using purified HC-AdV as a template for multiplex-qPCR after heat-inactivation for 5 min at 80°C. Multiplex-qPCR reactions were performed and analyzed as previously described[57] using a PrimeTime Gene expression Master Mix (IDT).

Mouse strains

Experiments were approved by the local ethics committee (Basel-Stadt, Switzerland) and performed in accordance with the Swiss federal regulations (Approval 3099). NSG mice (NOD.Cg-*Prkdc*^{scid} *Il2rg*^{tm1Wjl}/SzJ, RRID:IMSR_JAX:005557) were bred in-house at the University Hospital, Basel, Switzerland in pathogen-free, ventilated HEPA-filtered cages under stable housing conditions of 45%–65% humidity, a temperature of 21°C–25°C, and a gradual light–dark cycle with light from 7:00 a.m. to 5:00 p.m. Mice were provided with standard food and water without restriction (License: 1007-2H).

Patient samples

Buffy coats from healthy donors were obtained from the Blood Bank (University Hospital, Basel, Switzerland). Sample collection and use of corresponding clinical data was approved by the local ethics committee in Basel, Switzerland (Ethikkommission Nordwestschweiz, EKNZ, Basel-Stadt, Switzerland) and written informed consent was obtained from all donors before sample collection.

PBMC isolation

Human PBMCs were isolated from buffy coats by density gradient centrifugation using Hisopaque-1077 (Millipore, Burlington, MA) and SepMate PBMC isolation tubes (StemCell, Vancouver, Canada) according to the manufacturer's protocol, followed by red blood cell lysis using RBC lysis buffer (eBioscience, Santa Clara, CA) for 2 min at RT. Subsequently, cells were washed with PBS and ready for further analysis. Single cell suspensions were stored in liquid nitrogen until further use (in 90% FBS and 10% DMSO).

T cell isolation

Human T cells were isolated from frozen healthy donor PBMCs using the EasySep Human T cell isolation Kit (StemCell) according to manufacturer's instructions. Purity was tested by flow cytometry and was greater 95%. Freshly isolated T cells were rested overnight in RPMI Medium (Sigma-Aldrich) supplemented with 10% heat-inactivated fetal bovine serum (FBS; PAA Laboratories), 1x MEM non-essential amino acid solution (Sigma-Aldrich), 1 mM sodium pyruvate (Sigma-Aldrich), 0.05 mM 2-mercaptoethanol (Gibco), 1% penicillin/streptomycin (Sigma-Aldrich), and 50 IU of IL-2 (Proleukin, Iovance, San Carlos, CA).

Tumor models

To validate the anti-cancer efficacy of adenovirus-delivered DATE *in vivo*, we established a xenograft mouse model using female NOD/SCID mice that were injected subcutaneously with 3×10^6 human ovarian HER2-expressing SKOV3 cancer cells. Mice were between 8 and 12 weeks of age at the beginning of the experiment. The vector was administered intratumorally once the tumors reached a tumor volume of 30–100 mm^3. Each mouse received three doses of virus with 1.7×10^8 transducing units every 2–3 days. Mice that were treated with recombinantly produced DATE protein received three consecutive intratumoral injections of 1 μg DATE protein per administration every 2–3 days. Human T cells (7×10^6) isolated from healthy donors were injected intravenously 1 day after the first virus administration and 50 μL IL-2 (Proleukin Iovance) was given every week intraperitoneally at a dose of 2.75 mg/mL for 4 weeks. In the systemic administration experiment (Figure S7), mice were treated with three intravenous injections of DATE-AdV and a single, intravenous injection of 7×10^6 human T cells. The tumor size was assessed three times a week by caliper. Animals were euthanized before reaching a tumor volume of 1500 mm^3 or when reaching an exclusion criterion. The tumor volume was calculated according to the following formula: $V\ (mm^3) = (d^2 \times D)/2$ with D and d being the longest and shortest tumor diameter in mm, respectively.

Murine tumor and serum collection

For virus detection, tumors at endpoint were collected and either snap-frozen in liquid nitrogen or embedded in optimal cutting temperature (OCT) embedding matrix (CellPath, Newtown, UK). Samples were stored at −80°C until further use. For serum collection, blood from the tail vein of mice was collected 11 days after the first virus injection by tail vein puncture. Blood was transferred to a Microvette coated with EDTA (Microvette 200 K3E, Sarstedt, Nürmbrecht, Germany) and centrifugated at 10,000 × *g* for 5 min at RT. The collected serum was frozen for later analysis and stored at −80°C.

Immunohistochemistry

IHC was performed using cryosections (10 μm) of frozen tumor tissues embedded in OCT Embedding Matrix (CellPath). Cryosections were fixed with ice-cold acetone for 10 min, washed with IHC-PBS-T (PBS, pH 7.4, containing 0.1% [v/v] Tween 20), and blocked with IHC-blocking buffer (IHC-PBS-T with 10% normal goat serum [Cell Signaling Technology]) for 1 h at RT. Sections were incubated with primary antibody diluted in IHC-blocking buffer for 1 h at RT. After washing, sections were incubated with appropriate secondary antibody diluted in IHC-blocking buffer for 1 h at RT, washed, and counterstained with DAPI (Thermo Fisher Scientific; 300 nM final concentration) for 5 min at RT. After final washing, sections were mounted with ProLong Gold antifade mounting medium (Thermo Fisher Scientific) and analyzed using a THUNDER Imager Microscope (Leica, Wetzlar, Germany). Antibodies used for IHC analysis included mouse anti-human CD3-IgG-AF647 (BioLegend, 300416; 1:50), rabbit anti-DARPin serum (produced in-house; 1:100), and goat anti-rabbit IgG-AF555 (Thermo Fisher Scientific, A21429; 1:400).

DATA AND CODE AVAILABILITY

The data presented in this study are available upon reasonable request to the corresponding author A.P.

SUPPLEMENTAL INFORMATION

Supplemental information can be found online at https://doi.org/10.1016/j.omton.2024.200821.

ACKNOWLEDGMENTS

We are thankful to Fabian Weiss for scientific discussion, technical support, and assistance with the production and purification of recombinant protein and to Prof. Dr. Lubor Borsig for access to the fluorescence microscope. We would also like to thank Jonas Wepfer and Dr. Mark Hilge for assistance with creating the DATE model. We acknowledge the Flow Cytometry Facility of the University of Zurich for training of the users and maintenance of the instruments. We would like to thank the following funding agencies for supporting this work: the Swiss National Science Foundation Sinergia Grant CRSII5_170929 (to A.P.) and the University of Zurich Candoc Grant FK-20-031 (to J.K.). The graphical abstract was generated with BioRender.com.

AUTHOR CONTRIBUTIONS

Conceptualization: P.C.F., J.K., and A.P.; Methodology: P.C.F., J.K., R.Wieboldt, and R.Weber; Investigation: P.C.F., J.K., R.Wieboldt, R.Weber, K.P.H., and M.v.G.; Formal Analysis: P.C.F., J.K., and R.Wieboldt; Resources: P.C.F., J.K., R.Weber, and D.B.; Validation: P.C.F. and J.K.; Project Administration: P.C.F. and J.K.; Visualization: P.C.F., J.K., R.Wieboldt, R.Weber, and K.P.H.; Supervision: A.P.; Writing – Original Draft: P.C.F. and J.K.; Writing – Review & Editing: P.C.F., J.K.,

R.Wieboldt, K.P.H., M.v.G., D.B., H.L., and A.P.; Funding Acquisition: J.K., H.L., and A.P.

DECLARATION OF INTERESTS

A.P. is a co-founder and shareholder and D.B. is an employee and shareholder of Vector BioPharma, which is commercializing this technology. H.L. received travel grants and consultant fees from Bristol-Myers Squibb (BMS) and Merck, Sharp, and Dohme (MSD). H.L. received research support from BMS, Novartis, ONO Pharma, GlycoEra, and Palleon Pharmaceuticals. P.C.F., J.K., R.Wieboldt, H.L., and A.P. have filed a patent using the described technology.

REFERENCES

1. Huehls, A.M., Coupet, T.A., and Sentman, C.L. (2015). Bispecific T-cell engagers for cancer immunotherapy. Immunol. Cell Biol. *93*, 290–296.
2. Kebenko, M., Goebeler, M.E., Wolf, M., Hasenburg, A., Seggewiss-Bernhardt, R., Ritter, B., Rautenberg, B., Atanackovic, D., Kratzer, A., Rottman, J.B., et al. (2018). A multicenter phase 1 study of solitomab (MT110, AMG 110), a bispecific EpCAM/CD3 T-cell engager (BiTE®) antibody construct, in patients with refractory solid tumors. OncoImmunology *7*, e1450710.
3. Newman, M.J., and Benani, D.J. (2016). A review of blinatumomab, a novel immunotherapy. J. Oncol. Pharm. Pract. *22*, 639–645.
4. Pituch, K.C., Zannikou, M., Ilut, L., Xiao, T., Chastkofsky, M., Sukhanova, M., Bertolino, N., Procissi, D., Amidei, C., Horbinski, C.M., et al. (2021). Neural stem cells secreting bispecific T cell engager to induce selective antiglioma activity. Proc. Natl. Acad. Sci. USA *118*, e2015800118.
5. Brinkmann, U., and Kontermann, R.E. (2017). The making of bispecific antibodies. mAbs *9*, 182–212.
6. Goebeler, M.E., and Bargou, R.C. (2020). T cell-engaging therapies - BiTEs and beyond. Nat. Rev. Clin. Oncol. *17*, 418–434.
7. Baeuerle, P.A., and Reinhardt, C. (2009). Bispecific T-cell engaging antibodies for cancer therapy. Cancer Res. *69*, 4941–4944.
8. Wolf, E., Hofmeister, R., Kufer, P., Schlereth, B., and Baeuerle, P.A. (2005). BiTEs: bispecific antibody constructs with unique anti-tumor activity. Drug Discov. Today *10*, 1237–1244.
9. Klinger, M., Brandl, C., Zugmaier, G., Hijazi, Y., Bargou, R.C., Topp, M.S., Gökbuget, N., Neumann, S., Goebeler, M., Viardot, A., et al. (2012). Immunopharmacologic response of patients with B-lineage acute lymphoblastic leukemia to continuous infusion of T cell-engaging CD19/CD3-bispecific BiTE antibody blinatumomab. Blood *119*, 6226–6233.
10. Castelli, M.S., McGonigle, P., and Hornby, P.J. (2019). The pharmacology and therapeutic applications of monoclonal antibodies. Pharmacol. Res. Perspect. *7*, e00535.
11. Ovacik, M., and Lin, K. (2018). Tutorial on monoclonal antibody pharmacokinetics and its considerations in early development. Clin. Transl. Sci. *11*, 540–552.
12. Arvedson, T., Bailis, J.M., Britten, C.D., Klinger, M., Nagorsen, D., Coxon, A., Egen, J.G., and Martin, F. (2022). Targeting solid tumors with bispecific T cell engager immune therapy. Annu. Rev. Cancer Biol. *6*, 17–34.
13. Press, M.F., Cordon-Cardo, C., and Slamon, D.J. (1990). Expression of the HER-2/neu proto-oncogene in normal human adult and fetal tissues. Oncogene *5*, 953–962.
14. Florido, R., Smith, K.L., Cuomo, K.K., and Russell, S.D. (2017). Cardiotoxicity from human epidermal growth factor receptor-2 (HER2) targeted therapies. J. Am. Heart Assoc. *6*, e006915.
15. Baghban, R., Roshangar, L., Jahanban-Esfahlan, R., Seidi, K., Ebrahimi-Kalan, A., Jaymand, M., Kolahian, S., Javaheri, T., and Zare, P. (2020). Tumor microenvironment complexity and therapeutic implications at a glance. Cell Commun. Signal. *18*, 59.
16. Nakamura, K., and Smyth, M.J. (2020). Myeloid immunosuppression and immune checkpoints in the tumor microenvironment. Cell. Mol. Immunol. *17*, 1–12.
17. Fajardo, C.A., Guedan, S., Rojas, L.A., Moreno, R., Arias-Badia, M., de Sostoa, J., June, C.H., and Alemany, R. (2017). Oncolytic adenoviral delivery of an EGFR-targeting T-cell engager improves antitumor efficacy. Cancer Res. *77*, 2052–2063.
18. Freedman, J.D., Hagel, J., Scott, E.M., Psallidas, I., Gupta, A., Spiers, L., Miller, P., Kanellakis, N., Ashfield, R., Fisher, K.D., et al. (2017). Oncolytic adenovirus expressing bispecific antibody targets T-cell cytotoxicity in cancer biopsies. EMBO Mol. Med. *9*, 1067–1087.
19. Heidbuechel, J.P.W., and Engeland, C.E. (2021). Oncolytic viruses encoding bispecific T cell engagers: a blueprint for emerging immunovirotherapies. J. Hematol. Oncol. *14*, 63.
20. Brücher, D., Kirchhammer, N., Smith, S.N., Schumacher, J., Schumacher, N., Kolibius, J., Freitag, P.C., Schmid, M., Weiss, F., Keller, C., et al. (2021). iMATCH: an integrated modular assembly system for therapeutic combination high-capacity adenovirus gene therapy. Mol. Ther. Methods Clin. Dev. *20*, 572–586.
21. Porter, C.E., Rosewell Shaw, A., Jung, Y., Yip, T., Castro, P.D., Sandulache, V.C., Sikora, A., Gottschalk, S., Ittman, M.M., and Brenner, M.K. (2020). Oncolytic adenovirus armed with BiTE, cytokine, and checkpoint inhibitor enables CAR T cells to control the growth of heterogeneous tumors. Mol. Ther. *28*, 1251–1262.
22. Rosewell Shaw, A., Porter, C., Biegert, G., Jatta, L., and Suzuki, M. (2022). HydrAd: A helper-dependent adenovirus targeting multiple immune pathways for cancer immunotherapy. Cancers *14*, 2769.
23. Dreier, B., Honegger, A., Hess, C., Nagy-Davidescu, G., Mittl, P.R.E., Grütter, M.G., Belousova, N., Mikheeva, G., Krasnykh, V., and Plückthun, A. (2013). Development of a generic adenovirus delivery system based on structure-guided design of bispecific trimeric DARPin adapters. Proc. Natl. Acad. Sci. USA *110*, E869–E877.
24. Dreier, B., Mikheeva, G., Belousova, N., Parizek, P., Boczek, E., Jelesarov, I., Forrer, P., Plückthun, A., and Krasnykh, V. (2011). Her2-specific multivalent adapters confer designed tropism to adenovirus for gene targeting. J. Mol. Biol. *405*, 410–426.
25. Schmid, M., Ernst, P., Honegger, A., Suomalainen, M., Zimmermann, M., Braun, L., Stauffer, S., Thom, C., Dreier, B., Eibauer, M., et al. (2018). Adenoviral vector with shield and adapter increases tumor specificity and escapes liver and immune control. Nat. Commun. *9*, 450.
26. Smith, S.N., Schubert, R., Simic, B., Brücher, D., Schmid, M., Kirk, N., Freitag, P.C., Gradinaru, V., and Plückthun, A. (2021). The SHREAD gene therapy platform for paracrine delivery improves tumor localization and intratumoral effects of a clinical antibody. Proc. Natl. Acad. Sci. USA *118*, e2017925118.
27. Bhatta, P., and Humphreys, D.P. (2018). Relative contribution of framework and CDR regions in antibody variable domains to multimerisation of Fv- and scFv-containing bispecific antibodies. Antibodies *7*, 35.
28. Klein, C., Sustmann, C., Thomas, M., Stubenrauch, K., Croasdale, R., Schanzer, J., Brinkmann, U., Kettenberger, H., Regula, J.T., and Schaefer, W. (2012). Progress in overcoming the chain association issue in bispecific heterodimeric IgG antibodies. mAbs *4*, 653–663.
29. (2020). DARPins stack up as anti-COVID-19 agents Nat. Biotechnol. *38*, 1369. https://doi.org/10.1038/s41587-020-00771-w.
30. Binz, H.K., Amstutz, P., and Plückthun, A. (2005). Engineering novel binding proteins from nonimmunoglobulin domains. Nat. Biotechnol. *23*, 1257–1268.
31. Forrer, P., Binz, H.K., Stumpp, M.T., and Plückthun, A. (2004). Consensus design of repeat proteins. Chembiochem *5*, 183–189.
32. Plückthun, A. (2015). Designed ankyrin repeat proteins (DARPins): binding proteins for research, diagnostics, and therapy. Annu. Rev. Pharmacol. Toxicol. *55*, 489–511.
33. Stumpp, M.T., Dawson, K.M., and Binz, H.K. (2020). Beyond antibodies: the DARPin(®) drug platform. BioDrugs *34*, 423–433.
34. Boucher, L.E., Prinslow, E.G., Feldkamp, M., Yi, F., Nanjunda, R., Wu, S.J., Liu, T., Lacy, E.R., Jacobs, S., Kozlyuk, N., et al. (2023). "Stapling" scFv for multispecific biotherapeutics of superior properties. mAbs *15*, 2195517.
35. Zahnd, C., Wyler, E., Schwenk, J.M., Steiner, D., Lawrence, M.C., McKern, N.M., Pecorari, F., Ward, C.W., Joos, T.O., and Plückthun, A. (2007). A designed ankyrin repeat protein evolved to picomolar affinity to Her2. J. Mol. Biol. *369*, 1015–1028.
36. Chichili, G.R., Huang, L., Li, H., Burke, S., He, L., Tang, Q., Jin, L., Gorlatov, S., Ciccarone, V., Chen, F., et al. (2015). A CD3xCD123 bispecific DART for redirecting

host T cells to myelogenous leukemia: preclinical activity and safety in nonhuman primates. Sci. Transl. Med. *7*, 289ra282.

37. Björkelund, H., Gedda, L., Barta, P., Malmqvist, M., and Andersson, K. (2011). Gefitinib induces epidermal growth factor receptor dimers which alters the interaction characteristics with ^{125}I-EGF. PLoS One *6*, e24739.

38. Leyton, J.V. (2020). Improving receptor-mediated intracellular access and accumulation of antibody therapeutics - the tale of HER2. Antibodies *9*, 32.

39. Onsum, M.D., Geretti, E., Paragas, V., Kudla, A.J., Moulis, S.P., Luus, L., Wickham, T.J., McDonagh, C.F., MacBeath, G., and Hendriks, B.S. (2013). Single-cell quantitative HER2 measurement identifies heterogeneity and distinct subgroups within traditionally defined HER2-positive patients. Am. J. Pathol. *183*, 1446–1460.

40. Bulcha, J.T., Wang, Y., Ma, H., Tai, P.W.L., and Gao, G. (2021). Viral vector platforms within the gene therapy landscape. Signal Transduct. Target. Ther. *6*, 53.

41. Ricobaraza, A., Gonzalez-Aparicio, M., Mora-Jimenez, L., Lumbreras, S., and Hernandez-Alcoceba, R. (2020). High-capacity adenoviral vectors: expanding the scope of gene therapy. Int. J. Mol. Sci. *21*, 3643.

42. Freitag, P.C., Brandl, F., Brücher, D., Weiss, F., Dreier, B., and Plückthun, A. (2022). Modular adapters utilizing binders of different molecular types expand cell-targeting options for adenovirus gene delivery. Bioconjug. Chem. *33*, 1595–1601.

43. Freitag, P.C., Kaulfuss, M., Flühler, L., Mietz, J., Weiss, F., Brücher, D., Kolibius, J., Hartmann, K.P., Smith, S.N., Münz, C., et al. (2023). Targeted adenovirus-mediated transduction of human T cells in vitro and in vivo. Mol. Ther. Methods Clin. Dev. *29*, 120–132.

44. Hartmann, K.P., van Gogh, M., Freitag, P.C., Kast, F., Nagy-Davidescu, G., Borsig, L., and Plückthun, A. (2023). FAP-retargeted Ad5 enables in vivo gene delivery to stromal cells in the tumor microenvironment. Mol. Ther. *31*, 2914–2928.

45. Simão, D.C., Zarrabi, K.K., Mendes, J.L., Luz, R., Garcia, J.A., Kelly, W.K., and Barata, P.C. (2023). Bispecific T-cell engagers therapies in solid tumors: focusing on prostate cancer. Cancers *15*, 1412.

46. Ellerman, D. (2019). Bispecific T-cell engagers: towards understanding variables influencing the in vitro potency and tumor selectivity and their modulation to enhance their efficacy and safety. Methods *154*, 102–117.

47. Kroschinsky, F., Stölzel, F., von Bonin, S., Beutel, G., Kochanek, M., Kiehl, M., and Schellongowski, P.; Intensive Care in Hematological and Oncological Patients iCHOP Collaborative Group (2017). New drugs, new toxicities: severe side effects of modern targeted and immunotherapy of cancer and their management. Crit. Care *21*, 89.

48. Jost, C., Schilling, J., Tamaskovic, R., Schwill, M., Honegger, A., and Plückthun, A. (2013). Structural basis for eliciting a cytotoxic effect in HER2-overexpressing cancer cells via binding to the extracellular domain of HER2. Structure *21*, 1979–1991.

49. Chen, W., Yang, F., Wang, C., Narula, J., Pascua, E., Ni, I., Ding, S., Deng, X., Chu, M.L.H., Pham, A., et al. (2021). One size does not fit all: navigating the multi-dimensional space to optimize T-cell engaging protein therapeutics. mAbs *13*, 1871171.

50. Jung, S., Honegger, A., and Plückthun, A. (1999). Selection for improved protein stability by phage display. J. Mol. Biol. *294*, 163–180.

51. Röthlisberger, D., Honegger, A., and Plückthun, A. (2005). Domain interactions in the Fab fragment: a comparative evaluation of the single-chain Fv and Fab format engineered with variable domains of different stability. J. Mol. Biol. *347*, 773–789.

52. Wörn, A., and Plückthun, A. (2001). Stability engineering of antibody single-chain Fv fragments. J. Mol. Biol. *305*, 989–1010.

53. Hemminki, O., Dos Santos, J.M., and Hemminki, A. (2020). Oncolytic viruses for cancer immunotherapy. J. Hematol. Oncol. *13*, 84.

54. Pol, J.G., Workenhe, S.T., Konda, P., Gujar, S., and Kroemer, G. (2020). Cytokines in oncolytic virotherapy. Cytokine Growth Factor Rev. *56*, 4–27.

55. Day, C.P., Merlino, G., and Van Dyke, T. (2015). Preclinical mouse cancer models: a maze of opportunities and challenges. Cell *163*, 39–53.

56. Sandig, V., Youil, R., Bett, A.J., Franlin, L.L., Oshima, M., Maione, D., Wang, F., Metzker, M.L., Savino, R., and Caskey, C.T. (2000). Optimization of the helper-dependent adenovirus system for production and potency in vivo. Proc. Natl. Acad. Sci. USA *97*, 1002–1007.

57. Jager, L., Hausl, M.A., Rauschhuber, C., Wolf, N.M., Kay, M.A., and Ehrhardt, A. (2009). A rapid protocol for construction and production of high-capacity adenoviral vectors. Nat. Protoc. *4*, 547–564.